Overpressure generation and evolution in a compressional tectonic setting, the southern margin of Junggar Basin, northwestern China

Xiaorong Luo, Zhaoming Wang, Liqiang Zhang, Wan Yang, and Loujun Liu

ABSTRACT

Overpressure is widespread in the southern margin of the Junggar Basin, northwestern China. Pressure measurements in drillstem tests and repeated formation tests and estimates from wire-line logs indicate contrasting overpressure values between permeable sandstones and adjacent low-permeability mudrocks. In addition, excess pressure differs among anticlines with similar depth, lithologies, and geologic age, indicating significant lateral changes of overpressure. Major factors controlling overpressure generation and distribution include rapid sediment deposition, pressure compartmentalization by thick mudrocks, tectonic stress, faulting, and folding. Clay transformation and hydrocarbon generation are believed to be insignificant in overpressure generation in the southern Junggar Basin. Numerical modeling of pressure generation and evolution suggests that faulting and stratal tilting associated with folding are the most significant factors in the overpressure generation of a permeable sandstone. The extremely high overpressure (pressure coefficient up to 2.43) may have been caused by hydraulic adjustment within permeable sandstones associated with structural deformation caused by post-Miocene intense tectonic activities.

INTRODUCTION

Overpressure is common in the southern margin of the Junggar Basin, northwestern China, which has been subject to intense tectonic compression from the adjacent northern Tianshan (sometimes

Manuscript received April 17, 2006; provisional acceptance June 21, 2006; revised manuscript received February 6, 2007; final acceptance February 26, 2007.
DOI:10.1306/02260706035

AUTHORS

XIAORONG LUO ~ *Department of Geology, Northwest University, Xi'an 710069, China; present address: Key Laboratory of Petroleum Resources, Institute of Geology and Geophysics, Chinese Academy of Sciences, Beijing 100029, China; luoxr@mail.igcas.ac.cn*

Xiaorong Luo is a research scientist in the Chinese Academy of Sciences and has a B.S. degree and an M.S. degree in geology from Northwestern University, China, and a Ph.D. in geophysics from the University of Montpellier, France. His research in the last 20 years has been in petroleum geology, currently focusing on numerical modeling, geopressuring, and hydrocarbon migration and accumulation.

ZHAOMING WANG ~ *Key Laboratory of Petroleum Resources, Institute of Geology and Geophysics, Chinese Academy of Sciences, Beijing 100029, China*

Zhaoming Wang obtained a B.S. degree from the China University of Petroleum, Dongying, in 1998, and an M.S. degree in petroleum geology at the Institute of Geology and Geophysics, Chinese Academy of Sciences, in 2004. He has worked in the Shengli oil field. Currently, he is a Ph.D. student with interests in basin analysis, basin modeling, and hydrocarbon migration.

LIQIANG ZHANG ~ *Key Laboratory of Petroleum Resources, Institute of Geology and Geophysics, Chinese Academy of Sciences, Beijing 100029, China; present address: Faculty of Geo-Resources and Information, China University of Petroleum, Dongying, 257061, China*

Liqiang Zhang got a B.S. degree in 1994 and an M.S. degree in 1998 from the China University of Petroleum, Dongying, and a Ph.D. from the Institute of Geology and Geophysics, Chinese Academy of Sciences, in 2006. He is an associate professor of the Faculty of Geo-Resources and Information, the China University of Petroleum, Dongying. His research interests focus on sequence stratigraphy and sedimentology, as well as their applications in hydrocarbon exploration in continental basins.

WAN YANG ~ *Key Laboratory of Petroleum Resources, Institute of Geology and Geophysics, Chinese Academy of Sciences, Beijing 100029, China; present address: Department of Geology, Wichita State University, Wichita, Kansas 67260*

Wan Yang obtained a Ph.D. from the University of Texas at Austin in 1995 and is currently an associate professor at Wichita State University, teaching sedimentology and terrigenous clastic depositional systems. He has worked on depositional systems analysis, sequence and cyclostratigraphy, paleoclimatology, and reservoir characterization of marine and nonmarine siliciclastic and carbonate rocks in China and the United States.

LOUJUN LIU ~ *Research Institute of Exploration and Development, PetroChina Xinjiang Oil, Karamay, Xinjiang 834000, China*

Loujun Liu has a B.S. degree in geology from the China University of Petroleum, Dongying. He is now working in the Geophysical Research Institute of Geological Study Division of the Xinjiang Oil Administrative Bureau, conducting geological studies and management of oil and gas exploration. He researched initially on petroleum systems in petroliferous basins in China and has more than 20 years of exploration experience in the Junggar Basin. His research interests focus on geological conditions of hydrocarbon accumulation.

ACKNOWLEDGEMENTS

This study was supported partly by the Chinese National Major Fundamental Research Developing Project (2006CB202305) and by the Chinese National Natural Science Foundation (40072045), both to X. R. Luo. We thank *AAPG Bulletin* reviewers C. K. Morley, Q. M. Yang, Frances Whitehurst, and editor E. A. Mancini for thoughtful reviews. Computer modeling in this study was conducted using the Temis-2D, a basin-modeling computer software developed by the French Petroleum Institute (IFP).

spelled Tian Shan or Tien Shan) orogen in the south since the Miocene (Figure 1). Overpressure distribution is highly variable (Wu et al., 2000; Zeng et al., 2000); the pressure coefficient is commonly larger than 2.0 and up to 2.43, and in some cases, hydrostatic pressures were encountered. Wu et al. (2000) and Li et al. (2001) suggested that the high overpressure is closely related to pressure compartmentalization by thick mudrocks in the Eocene–Oligocene Anjihaihe Formation (Figure 2). Some workers (e.g., Kuang, 1993; Wu et al., 2000; Xu et al., 2000; Li et al., 2001; Li, 2004) paid more attention to the rapid sediment deposition since the Pliocene and northward compression from the northern Tianshan, in addition to factors such as thermal expansion of pore water, dehydration during smectite-to-illite and gypsum-to-anhydrite transformations, and hydrocarbon generation. Nevertheless, overpressure distribution was not fully understood because of limited data, and the pressure difference between sandstone and mudrock was overlooked. Thus, the processes and mechanisms of overpressure generation in the southern Junggar Basin remain qualitative and speculative.

Quantitative analysis of overpressuring mechanisms in the last two decades suggests that some of them need to be reevaluated (Bethke, 1986; Luo and Vasseur, 1992; Osborne and Swarbrick, 1997), and some new mechanisms have been proposed (Luo and Vasseur, 1992; Yardley and Swarbrick, 2000; Luo et al., 2003). For example, thermal expansion of pore water (Luo and Vasseur, 1992; Osborne and Swarbrick, 1997), pore-water volume increase because of clay mineral transformation (Bethke, 1986), and hydrocarbon generation in source rocks with a total organic carbon (TOC) of less than 10% (Luo and Vasseur, 1996) have been proven to be insignificant in generating overpressure. However, fluid sourced from the underlying sedimentary strata during diagenesis (Luo and Vasseur, 1996), lateral pressure transmission along dipping permeable strata (Yardley and Swarbrick, 2000), and hydrodynamic connection of different pressure systems through episodic fault opening (Luo et al., 2003) can generate very high overpressure.

In this article, we characterized overpressure distribution in the Cenozoic sedimentary rocks in the southern margin of the Junggar Basin, evaluated the functions of geological factors in overpressure generation based on our understanding of the compressional tectonic history and its effect on overpressure distribution, and finally, simulated the processes of overpressure generation and evolution in the basin through quantitative modeling. Our study suggests that the extremely high overpressure on anticlines may have been caused by hydraulic adjustment within permeable sandstones during post-Miocene intense tectonic activities.

GEOLOGICAL BACKGROUND

The Junggar Basin in northwestern China contains upper Paleozoic, Mesozoic, and Cenozoic sedimentary deposits. Its southern margin, bounded by the northern Tianshan orogen and covering an area of

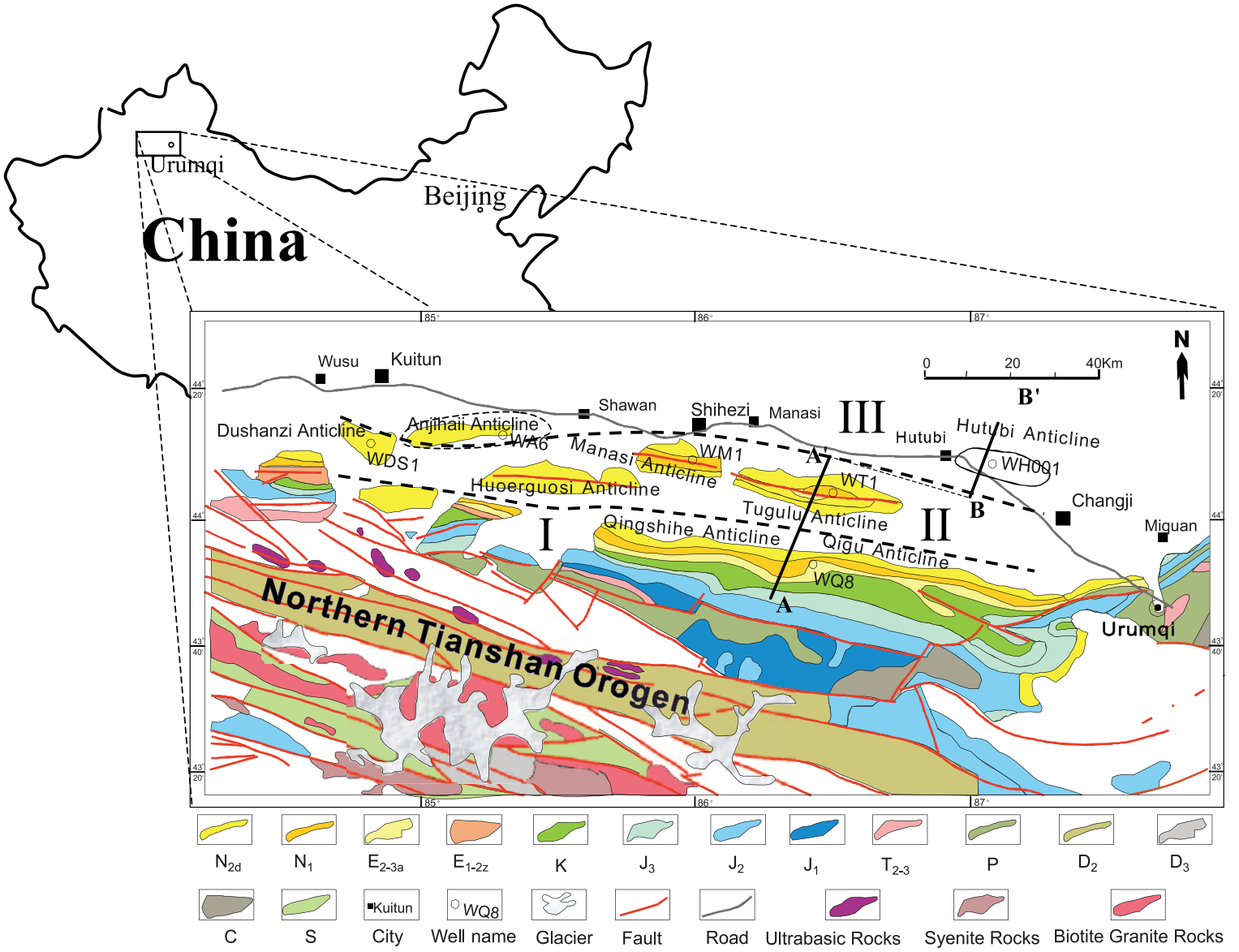

Figure 1. Location and structural grain of the southern margin of the Junggar Basin adjacent to the northern Tianshan orogen, northwestern China. Anticlines form three belts, which are marked as I, II, and III, and are demarcated by dashed lines. AA′ and BB′ are locations of seismic sections in Figure 7A and B. In the legends, N_{2d} = Pliocene Dushanzi Formation; N_1 = lower Neogene; E_{2-3a} = middle–upper Eocene basal Oligocene Anjihaihe Formation; E_{1-2z} = lower–middle Eocene Ziniquanzi Formation; K = Cretaceous; J_3 = Upper Jurassic; J_2 = Middle Jurassic; J_1 = Lower Jurassic; T_{2-3} = Middle–Upper Triassic; P = Permian; D_2 = Middle Devonian; D_3 = Upper Devonian; C = Carboniferous; S = Silurian (see also Figure 2).

Chrono- and Litho-stratigraphy					Thickness (m)	Major lithology
Erathem	System	Series	Formation	Symbol		
CENOZOIC	QUATERNARY	Pleisto-cene	Xiyu	Q_1x	1250 – 2470	Gray conglomerate and reddish brown shaly sandstone. A thin sandy mudrock at base.
	TERTIARY	Pliocene	Dushanzi	N_2d	1300–2000	Grayish green shale intercalated with sandstone and skeletal limestone.
		Miocene	Taxihe	N_1t	250–300	Reddish brown sandy shale and shaly sandstone intercalated with grayish green sandstone and calcite-cemented conglomerate.
			Shawan	N_1s	150–500	Maroon sandy shale interbedded with grayish green lenticular conglomerate and sandstone. Common calcitic nodules and concretions.
		Oligocene	Anjihaihe	$E_{2-3}a$	130–780	Grayish green, gray-black shale with skeletal limestone in the west; variegated mudstone and siltstone intercalated with sandy conglomerate in the east.
		Eocene	Ziniquanzi	$E_{1-2}z$	50–400	Maroon sandy shale with gray conglomerate. Some calcitic nodules.
MESOZOIC	CRETACEOUS	Upper	Donggou	K_2d	0–800	Maroon sandy shale and sandstone.
		Lower	Lianmuqin	K_1l	680–2000	Maroon sandy shale intercalated with grayish green fine sandstone.
			Shengjinkou	K_1s		Grayish green mudstone interbedded with sandstone containing ferruginous nodules.
			Hutubihe	K_1h		Sandy shale and sandstone overlying interbedded mudstone and sandstone.
			Qingshuihe	K_1q		Grayish green interbedded mudstone and sandstone. Conglomerate at base.
	JURASSIC	Upper	Kalazha	J_3k	0–850	Maroon conglomerate in the south and grayish green sandstone in the north.
			Qigu	J_3q	580–970	Maroon mudstone and sandstone.
		Middle	Toutunhe	J_2t	170–750	Variegated mudstone, sandy mudstone, and sandstone. Some coal seams.
			Xishanyao	J_2x	300–1100	Grayish green sandstone and mudstone intercalated with conglomerate. Abundant coal seams.
		Lower	Sangonghe	J_1s	220–810	Grayish green mudstone intercalated with thin sandstone and limestone
			Badaowan	J_1b	260–850	Sandy mudstone and sandstone with common coal seams overlying gray sandstone intercalated with mudstone. Conglomerate at base.
	TRIASSIC	Upper and Middle	Haojiagou Huangshanjie Kelamayi	$T_{2-3}xq$	800–1000	Grayish green sandstone, conglomerate, variegated mudstone, and sandy mudstone intercalated with thin ferruginous carbonate rocks.
		Lower	Shangcang fanggou	T_1ch	312–706	Purplish red conglomerate intercalated with mudstone; uppermost yellow sandstone
PALEOZOIC	PERMIAN	Upper	Quanzijie	P_2ch	300–650	Purplish red conglomerate intercalated with sparse sandy mudstone.
			Hongyanchi	P_2h	300–733	Grayish green, gray-black mudstone and shale intercalated with grayish green sandstone. Thin limestones in the middle part.
			Lucaogou	P_2l	90–1102	Gray-black shale and oil shale intercalated with dolomitic limestone in the upper part; black-brown medium-fine sandstone and sandy shale intercalated with oil shale with ferruginous nodules in the lower part.
			Jingjingzigou	P_2j	890	Grayish green sandstone and mudstone, with sparse tuffaceous sandstone and mudstone.
			Wulabo	P_2w	1374	Grayish green feldspathic sandstone, lithic sandstone, and siltstone.
		Lower	Xiajijicaozi	P_2jj	718–1721	Grayish green fine-grained lithic wackestone, siltstone, wavy-bedded limestone, carbonaceous shale, and minor felsite.

Figure 2. Upper Paleozoic, Mesozoic, and Cenozoic sedimentary strata in the southern margin of the Junggar Basin. The range of thickness and a brief lithologic description of individual formations and groups are given. The symbols of formations and groups are referred to in later figures. Wavy lines under formation and symbol columns indicate major unconformities.

230×50 km^2 (143×31 mi^2) (Figure 1), has experienced four orogenies (Hercynian, Indosinian, Yanshanian, and Himalayan) since the Permian, which are believed to have controlled basin development and the types and distribution of sedimentary facies (Figure 2).

Stratigraphy

More than 2000 m (6600 ft) of shallow-marine quartz arenite and mudrock were deposited in the eastern part of the southern margin of the Junggar Basin during the

Early Permian (Figure 2). The basin transformed into an intercontinental basin in the Late Permian (Cai et al., 2000). It experienced repeated uplifting and subsidence in the Early Triassic and became a shallow lacustrine basin during the Middle to Late Triassic, where about 1200 m (3900 ft) of mudrock and sandstone were deposited in the eastern part of the southern margin (Cai et al., 2000).

Coal beds are abundant and extensive in the Lower to Middle Jurassic deposits (Figure 2). Individual coal beds are up to tens of meters thick and interbedded with lacustrine and fluvial sandstones and mudrocks. The lower Middle Jurassic Xishanyao Formation was variably eroded and unconformably overlain by the upper Middle Jurassic Toutunhe Formation, caused by the northward compression and resulting folding. Cretaceous deposits are thick (>3000 m; >10,000 ft) in the east-central part of the southern margin and contain interbedded mudrock and sandstone and a basal conglomerate (Figure 2).

More than 1500 m (4900 ft) of mudrocks, sandstones, and conglomerates were deposited in a frontal depocenter in the central part of the southern margin during the Paleogene (Figure 2). The Paleocene–Eocene Ziniquanzi Formation, composed of sandstone intercalated with mudrocks, is thickest in the central-east part, thinning toward the east and west. Lateral facies change is common, and sediment preservation is variable. The Eocene–Oligocene Anjihaihe Formation is composed of very thick (tens to hundreds of meters) shale intercalated with limestone in the middle part and thin interbedded mudrock and sandstone in the lower and upper parts, which were deposited in a shallow to deep littoral lacustrine environment.

From the Miocene to the Quaternary, frontal depressions formed by northward thrusting and loading of the northern Tianshan caused by plate collision between India and Eurasia. The depocenter has migrated westward to the western end of the southern margin. The Miocene deposits are mainly fluvial-lacustrine mudrocks intercalated with sandstone, conglomerate, and limestone. The Pliocene deposits are mainly alluvial-fan to fluvial mudrock and sandstone intercalated with conglomerate. The Quaternary deposits are alluvial-fan to fluvial conglomerate and sandstone.

Structure

The structural characteristics and tectonic evolution of the southern margin of the Junggar Basin are closely related to the northern Tianshan orogen. The first episode of uplift and folding and accompanying volcanism in the northern Tianshan occurred in the Permian period and caused a continuous basin subsidence and deposition of thick sediments along the Tianshan front. Extension that dominated during orogenies occurred in the Mesozoic, forming grabens and horsts. Gradual uplifting of the northern Tianshan started again during the Late Cretaceous, and intense uplifting occurred during the Cenozoic. Northward thrusting and loading formed a foreland basin containing three east-west–oriented fold belts in the southern margin (Figures 1, 3).

The decollement surfaces within the Jurassic coal-bearing strata controlled the overall overthrusting tectonics in the southern Junggar, as indicated by the characteristics of Mesozoic–Cenozoic faults and folds (Figure 3). Anticlines are generally arranged in an en echelon pattern, and their northern limbs are generally steeper than the southern limbs. Rocks exposed on individual anticlines become younger from Mesozoic to Cenozoic basinward to the north. The first fold belt, which is the closest to the northern Tianshan, includes 11 anticlines formed within the Mesozoic rocks by transpressional overthrusting during the Late Cretaceous and Cenozoic orogenies (Wu et al., 2000). The second belt includes four major anticlines characterized by stratal overturning and thin-skinned overthrusting above a gravity-induced decollement along the ductile mudrock interval of the Eocene–Oligocene Anjihaihe Formation (Figure 3). The folds are sinistrally en echelon in the east and dextrally en echelon in the west. The third belt includes five open and elongate anticlines.

Tectonic Stress Field

Structural characteristics indicate that the Cenozoic tectonic stress field is characterized by approximately north-south or south-southwest–north-northeast horizontal compression, where horizontal maximum principal stress (σ_{hmax}) > vertical intermediate principal stress (σ_v) > horizontal minimum principal stress (σ_{hmin}) (Wu et al., 2000). A similar stress field was interpreted through earthquake fault-plane analysis (Nelson et al., 1987): the maximum principal stress is oriented mostly north-south or north-northeast–south-southwest (1–15°), with a near-horizontal inclination (generally <25°); the intermediate principal stress is vertical, and the minimum principal stress is nearly horizontal, all indicating a reverse fault motion. Earthquake surface fractures indicate a modern nearly north-south compressional stress field (Deng et al., 2000).

Such a stress field has resulted from the long-distance effect of the intense India–Eurasian plate collision (Cai

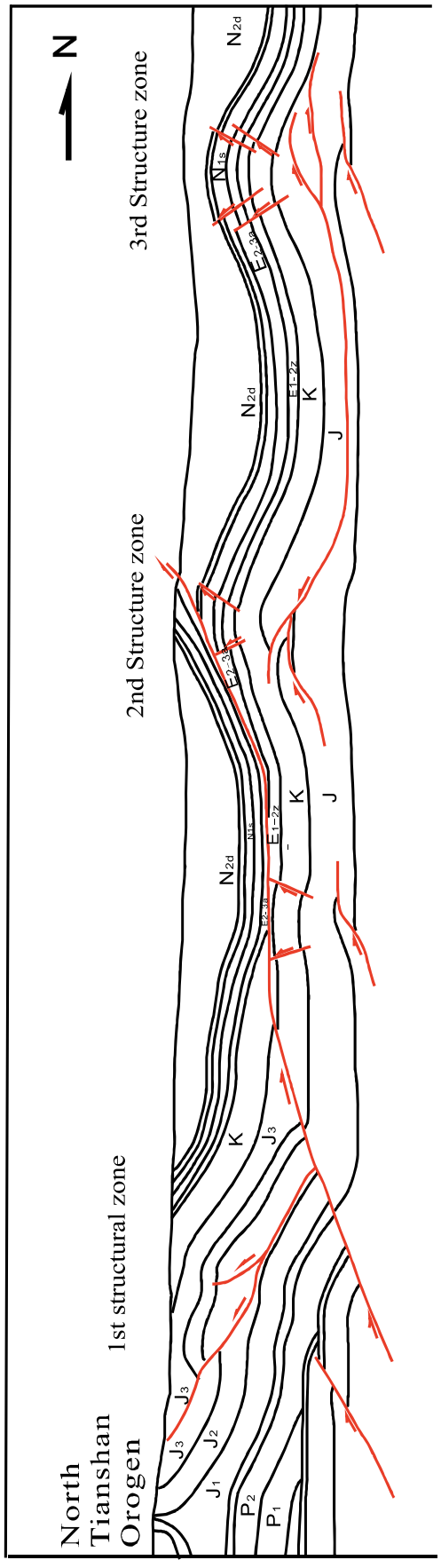

Figure 3. A north-south structural cross section showing the major structural styles as characterized by the three fold belts in the southern margin of the Junggar Basin. See Figure 2 for explanations of stratigraphic symbols.

et al., 2000). Global positioning system (GPS) measurements of the crustal velocity field in China and its vicinity (Li et al., 2001) indicated that the Tarim Basin, a microplate located south of the northern Tianshan orogen, has a northward motion, causing north-south compression of the Junggar Basin. Finally, GPS measurements of crustal movement in the Dushanzi area just west of the study area from 1995 to 1997 (Yin et al., 1999) indicated that the Tianshan region has a northward horizontal motion at a rate of 0.6–0.9 mm/yr (0.023–0.035 in./yr), conformable with the overall modern stress filed of western China (Ding et al., 1991).

OVERPRESSURE DISTRIBUTION IN THE SOUTHERN MARGIN OF THE JUNGGAR BASIN

Pressure measurements in wells indicate common overpressure and complex pressure distribution in the southern Junggar Basin (Figure 4). The mudstone compaction curves (Figure 4) indicate variable degrees of compaction. Undercompacted intervals, especially the middle and upper parts of the Anjihaihe Formation, commonly correlate with regionally persistent thick mudrock intervals. The pressure distribution in sandstones differs significantly from that of mudstones (Figure 4). Commonly, the measured pressure in sandstones (pressure coefficients >2.0) is much higher than that in the adjacent mudrocks (calculated pressure coefficients commonly <1.6). Pressure within individual sandstone pressure systems separated by regional mudrock intervals has a regular distribution pattern (Figure 5). For example, overpressure in the lower part of the Anjihaihe Formation and the subjacent Ziniquanzi Formation is extremely high and increases with depth following the hydrostatic gradient (Figure 5), whereas overpressure in the Shawan Formation overlying the Anjihaihe Formation is small and irregular. Some deep wells penetrated the Cretaceous Donggou Formation and possibly the underlying Tugulu Group, where even higher overpressure was measured (e.g., Figure 5). This particular pressure distribution suggests that overpressure within a sandstone system was not only transmitted from adjacent mudstones, but also supplied by other sources (e.g., Luo et al., 2000; Yardley and Swarbrick, 2000).

Areal pressure distribution differs within and between the three fold belts. In general, overpressure is high in the west and low in the east, the highest in the third (most basinward) belt and the lowest in the first mountain-front belt (Figures 1, 6). To eliminate the effect of burial depth on pore pressure, the excess

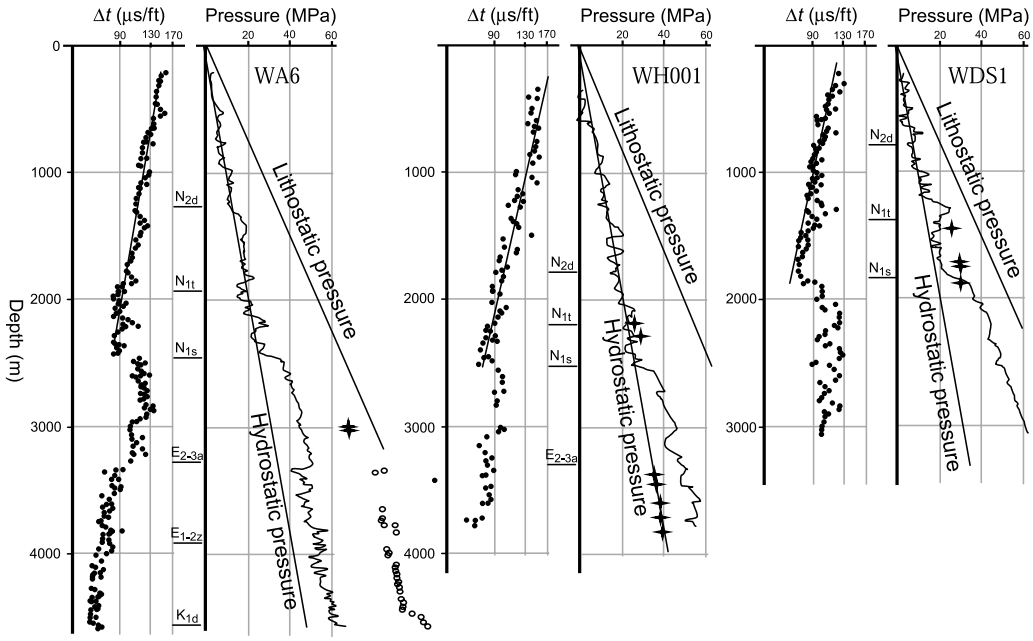

Figure 4. Mudstone compaction and pressure distribution in wells WA6, WH001, and WDS1 in the southern margin of the Junggar Basin, indicating common overpressure and complex pressure distribution. For each well, the left panel shows the interval time data points (filled dots) of mudrocks on acoustic logs reflecting trends of normal and undercompaction of mudrocks. The right panel shows the pressure distribution in mudrocks as estimated from acoustic logs (curved line), DST (drillstem test) measurements in permeable rocks (stars), RFT (repeat formation tests) measurements (open dots), and calculated lithostatic and hydrostatic pressures. A lithostatic pressure coefficient (2.45) was estimated from density logs of the strata above the undercompacted Anjihaihe Formation; a hydrostatic pressure coefficient of 1.0 is assumed; and the pressure within mudstone intervals is calculated using the balanced-depth method (Fertl, 1976; Magara, 1978). See Figure 1 for well location and Figure 2 for explanations of stratigraphic symbols.

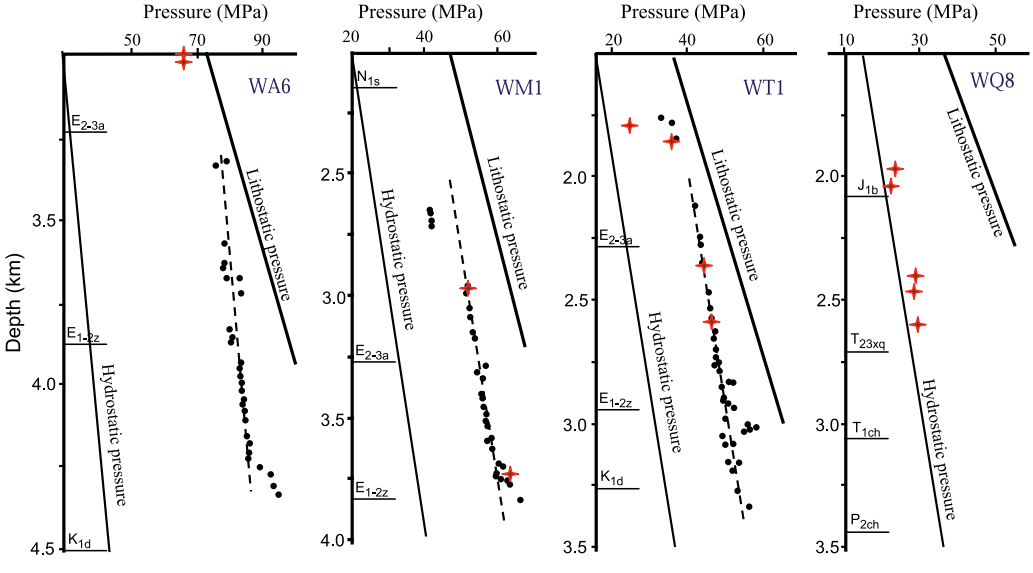

Figure 5. Distribution of pressure measured in DSTs (stars) and RFTs (dots) in wells WA6, WM1, WT1, and WQ8 in the southern margin of the Junggar Basin. The increase of overpressure with depth (dashed line) has the same gradient as that of hydrostatic pressure, suggesting that the shallow and deep pressure systems are unified and connected. See Figure 1 for well location and Figure 2 for explanations of stratigraphic symbols.

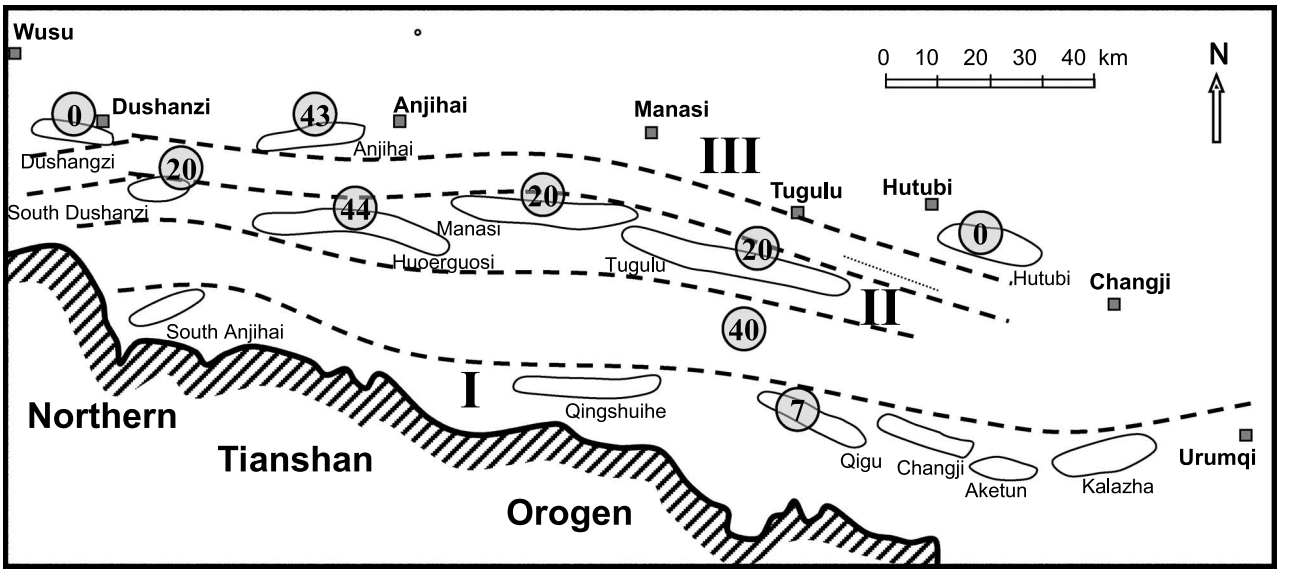

Figure 6. Distribution of maximum excess pressure measured in the Eocene Ziniquanzi and Eocene–Oligocene Anjihaihe formations (Figure 2) in the southern margin of the Junggar Basin. The large excess pressure indicates intact sealing of the upper Anjihai mudrocks, whereas the small and zero excess pressure indicates broken sealing where originally overpressured deep systems are connected to the shallow hydrostatically pressured systems.

pressure, the pressure difference between pore pressure and hydrostatic pressure, was used to compare the magnitude of overpressure on each anticline. In the first fold belt, Mesozoic strata have been exposed due to erosion since the Pliocene, so the present-day pressure measurements are not the maximum values that existed in the geologic history. On the Manas and Tugulu anticlines in the eastern and middle part of the second fold belt, respectively, excess pressure measured in the lower part of the Anjihaihe Formation is similar, whereas on the Huoerguosi anticline in the west, extreme overpressure of 74.5 MPa (with an excess pressure of 44.0 MPa) was measured in drillstem tests (DSTs) at a depth of 3070 m (10,072 ft). A similar pattern is present in the third fold belt. In well WA6 on the Anjihai anticline in the west, a pressure coefficient of 2.4 (corresponding to an excess pressure of 43 MPa) was measured in a repeat formation test (RFT) in the lower part of the Anjihaihe Formation, whereas on the Hutubi anticline to the east, the pressure in the same formation and the underlying strata is close to hydrostatic pressure (Figure 6).

OVERPRESSURING MECHANISMS IN THE SOUTHERN MARGIN OF THE JUNGGAR BASIN

The complex pressure distribution in the southern Junggar Basin cannot be satisfactorily explained by mechanisms proposed by previous workers (see Introduction section). To depict the origin and forming mechanisms of overpressure, the effects of intense tectonic activities since the Pliocene, which may have greatly changed the depositional conditions, structural styles, and fluid flows in the strata, need special consideration.

Fast Sediment Deposition

Fast sediment deposition is an important cause of overpressure (Chapman, 1980; Audet and McConnell, 1992) because it commonly hampers efficient porewater expulsion during sediment compaction (Magara, 1978; Swarbrick and Osborne, 1998). Bethke's (1986) study suggested that overpressure commonly occurs in basins where the depositional rate is greater than 100 m/m.y. (328 ft/m.y.) and where mudstone content is greater than 85%, such as the Cenozoic Gulf of Mexico Basin.

The depositional rate in the southern margin of the Junggar Basin since the Pliocene has been very high, up to 1000 m/m.y. (3280 ft/m.y.) in synclines (Figure 3). Thus, overpressure could form easily in the Anjihaihe and Taxihe formations, which contain thick mudrocks. Based on Audet and McConnell (1992), the overpressuring coefficient $\lambda = (V/K - 1)$ (where V is the depositional rate, and K is the hydraulic conductivity of mudrocks) in these two formations was estimated to be close to 0.1; thus, pressure increase with depth in

the two formations should closely follow the lithostatic pressure gradient.

On anticlines, however, overpressure generation caused by fast deposition was concurrent with tectonic uplift and surface erosion, which will lower the pressure within mudrocks (Neuzil and Pollock, 1983; Luo and Vasseur, 1996). This is indicated by the relatively low-pressure coefficient (commonly ~1.5), which was estimated from acoustic log data, in mudrocks on anticlines (Figure 5).

Pressure Sealing by Thick Mudrocks

Overpressure also occurs in basins with a small depositional rate (Law and Dickinson, 1985; Spencer, 1987; Mudford and Best, 1989), where the small rate is compensated by the presence of low-permeability mudrocks that significantly retard fluid expulsion to generate overpressure. Mudford and Best's (1989) model results suggest that significant overpressure can be generated within mudrocks less than 50 m (164 ft) thick. The thicknesses of individual mudrock intervals of the Anjihaihe Formation in wells Hu-2, An-4, and Xi-4 all exceed 100 m (328 ft) and, especially, reach 223 m (731 ft) in well WDS-1. These thick mudrock intervals undoubtedly are conducive to overpressure generation and preservation, as indicated by the significant undercompaction in the Anjihaihe Formation (Figure 4). In addition, the thick mudrocks are laterally persistent, forming regional cap rocks. These mudstones are generally pressure barriers and are so flexible because of overpressuring that even intense faulting could not destroy their sealability. Faulting may have caused hydrodynamic connectivity among sandstone bodies, but the connectivity is confined between the mudrock barriers, which partition the pressure field along depth.

Tectonic Stressing

Some attention has been paid to the function of tectonic stress in overpressure generation (Davis et al., 1983; Byerlee, 1990, 1993; Neuzil, 1995). The effect of tectonic stress is analogous to that of stratal overburden, which causes mudrock compaction and a decrease in porosity and permeability, resulting in retardation of fluid expulsion and overpressure generation.

The southern Junggar margin has experienced two major episodes of compression. The first episode was from the Pennsylvanian to Early Permian (Cai et al., 2000) and had no effect on the current overpressure. The second episode was during the Cenozoic, especially post-Miocene, and has contributed significantly to the current overpressure buildup. For example, acoustic test data of cores from well WH001 indicate that at 3180 m (10,433 ft), the horizontal maximum principal stress (115.52 MPa) > vertical overburden lithostatic pressure (77.39 MPa) > horizontal minimum principal stress (55.41 MPa). A 111.52-MPa tectonic stress is equivalent to 4746.8 m (15,573.5 ft) of stratal overburden. Thus, the combined effect of tectonic stress and overburden on sediment compaction will cause a much greater porosity and permeability reduction than the overburden alone and, as a result, greater retardation of fluid expulsion, which will generate overpressure at this depth.

Faulting

The abundant faults in the study area (Figure 3) have a wide depth range and might have hydrodynamically connected different overpressure systems. When two pressure systems are connected by an open fault, fluid pressure will adjust rapidly to reach hydrostatic balance and form a new pressure system (Grauls and Baleix, 1994; Luo et al., 2003). Within the new system, individual permeable strata will have the same excess pressure and fluid pressure increases with depth at the hydrostatic gradient, but the largest pressure coefficient should be in the shallow strata (Luo et al., 2003).

Overpressure in shallow permeable rocks hydrodynamically connected with a deep overpressure system can only be generated when the excess pressure in the deep system is larger than that of the shallow system. The shallow overpressure is sourced from the deep system. Thus, the extreme sealing condition is not needed to generate and to maintain high pressures within the shallow system when the deep system contains a large enough volume of fluid. During overpressure generation in the shallow system, the adjacent low-permeability mudrocks commonly serve as a fluid-flow barrier only and have a lower pore-water pressure than the permeable sandstones of the system (Figure 5). This mechanism of overpressure generation in shallow permeable strata explains well the high-pressure coefficients (up to 2.43) measured in the permeable strata (Figure 4) and the estimated low-pressure coefficients (equal to or less than 1.7) in the adjacent mudrocks (Figure 5) on the Huoerguosi and Anjihai anticlines.

Moreover, if the open fault fractures the seal of an overpressured system to connect the system with an overlying normal-pressured hydrostatic system, fluid flow

will cause pressure adjustment between the overpressured and hydrostatic systems, and eventually, both systems will become hydrostatic. On the Hutubi anticline, for example, the measured pressure in the permeable strata underlying mudrocks of the Anjihaihe Formation is hydrostatic, whereas the mudrocks themselves are undercompacted (Figure 4, WH001). That is, overpressure in the deep permeable strata is not present, although many geological conditions for overpressure generation on this anticline are similar to those on the Anjihai anticline. This is because faults on the Hutubi anticline have connected the originally overpressured deep system to shallow hydrostatic systems. Note that the connecting fault(s) may not be observed on wide-spaced seismic sections and may not have destroyed the hydrocarbon traps on the Hutubi anticline because the pressure field is three-dimensional.

Folding

Increasing surface erosion on an anticline should result in a rapid decrease of subsurface pressure (Neuzil and Pollock, 1983; Luo and Vasseur, 1996). This is, however, not true in the study area, where very high pressure was measured on anticlines. Lateral continuity and connectivity of permeable beds may be the key to explain this phenomenon (Yardley and Swarbrick, 2000). If a laterally persistent and dipping permeable bed on an anticline is hydrodynamically sealed in the updip part and extends downdip into an overpressure zone, the bed will receive fluid and pressure transmitted from the adjacent overpressured mudrocks. The transmitted pressure, however, varies along the permeable bed because excess pressure within the mudrocks is variable (Yardley and Swarbrick, 2000). However, excess pressure is the same in the permeable bed because it has a high hydraulic conductivity to quickly readjust uneven pressure distribution. As a result, a larger pressure coefficient and higher overpressure exist in the shallow updip part of the permeable bed than in the downdip part.

Folding is common in the study area and has two major effects on pressure generation and distribution: First, the amount of overburden varies horizontally, and thus, the burial rate, which is an important factor for overpressure generation, is different. Second, the burial depth of a permeable bed varies laterally, and therefore, the bed is in contact with adjacent, low-permeability rocks of different excess pressure. As a result, lateral fluid flow and pressure transmission within the tilted permeable bed will certainly occur (Yardley and Swarbrick, 2000). The pressure difference between the permeable bed and the adjacent low-permeability beds varies with structural positions. In synclines, overpressure would likely occur first in mudrocks because of the deep burial and would be transmitted into adjacent sandstones. On anticlines, overpressure would likely occur first in sandstones by lateral pressure transmission from the downdip part of the sandstones and, then, may be transmitted into the adjacent normally compacted mudrocks.

Other Overpressuring Mechanisms

Zha et al. (2000) suggested that hydrocarbon generation might have contributed to overpressure generation in the southern Junggar margin. The contribution is probably insignificant. Bethke (1986), Audet (1995), Luo and Vasseur (1996), and Osborne and Swarbrick (1997) all suggested that a significant amount of excess fluid pressure can be generated through hydrocarbon generation only when the TOC content in a source rock is very high. Luo and Vasseur's (1996) model results suggest that the TOC content in a source rock should be larger than 10% if only liquid hydrocarbons were generated, and 1% if gas were generated when organic matter cracking would induce significant excess pressure. The TOC content in the Cenozoic rocks in the southern Junggar Basin, however, is generally less than 1%, and the thermal maturation did not reach the peak of hydrocarbon generation. For example, R_o values from the Taxihe, Anjihaihe, and Ziniquani formations in wells Du-1 and WDS-1 are only 0.55, 0.44, and 0,73%, respectively. Hence, hydrocarbon generation probably is not a major factor in overpressure generation within the Cenozoic strata in the southern Junggar Basin.

However, the thick (hundreds of meters) multiple Jurassic coal beds are thermally mature with an R_o (vitrinite reflectance) of 1.3%. The generated natural gas should have produced fairly high overpressure. The overpressure is compartmentalized by the overlying extremely thick low-permeability Cretaceous strata (Figure 2) to form a deep overpressure system. Pressure in this system may have been transmitted to the shallow Tertiary overpressure system via open faults. However, Mesozoic rocks are exposed in the frontal Tianshan and have not been penetrated in the second and the third anticline belts. The characteristics and distribution of the deep pressure system await further study.

Pore-fluid pressure increase may also be caused by the addition of pore water during clay mineral

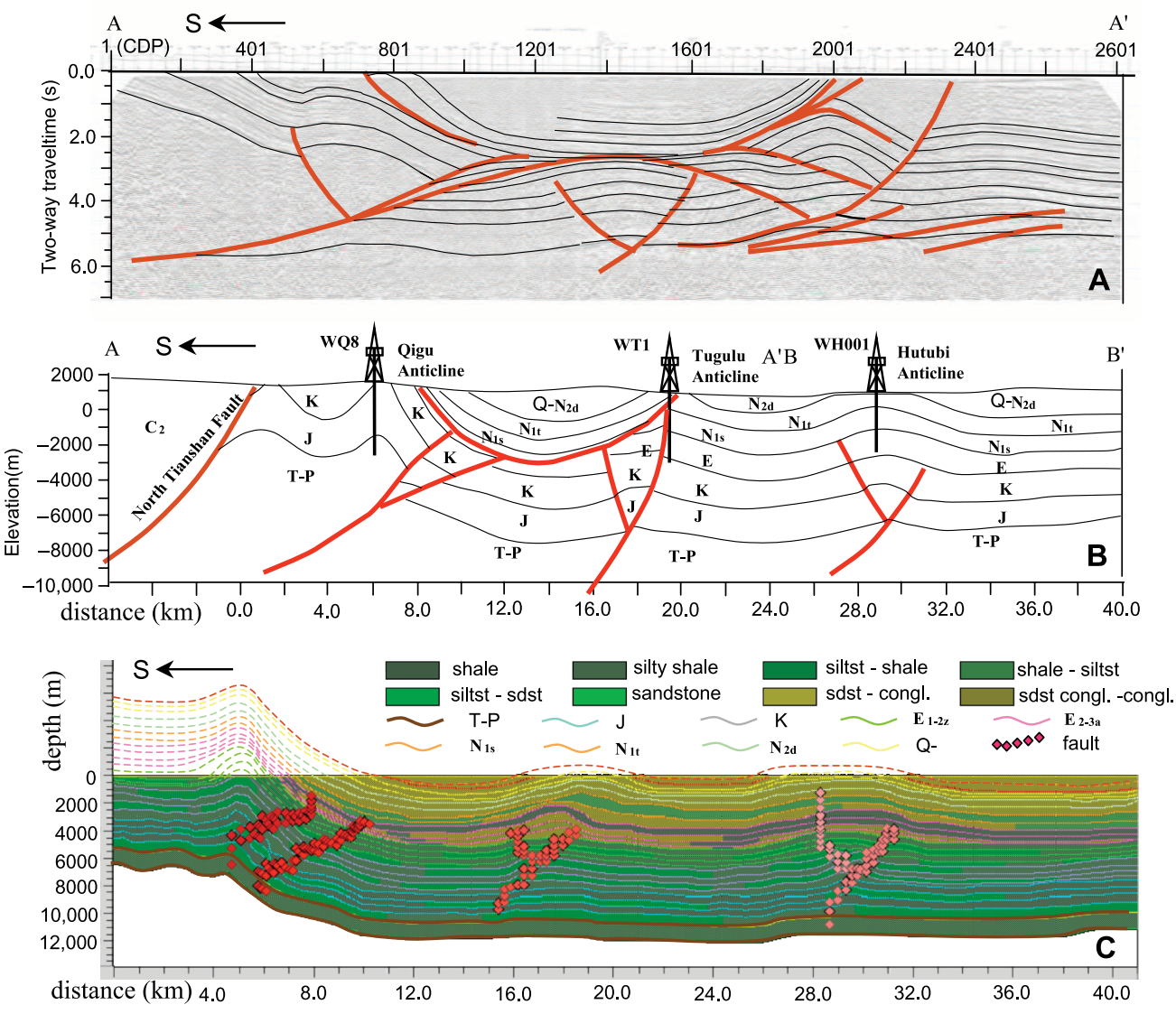

Figure 7. An example showing the steps in establishing a 2-D geological model for pressure simulation. (A) Seismic section AA′ with structural and stratigraphic interpretations (see Figure 1 for location). (B) A geological cross section constructed on the basis of seismic and well interpretations. Seismic sections AA′ and BB′ are joined along the depositional and structural strike to form the composite section (see Figure 1 for location). (C) Simplified geological cross section that can be accepted by the simulation software (see Acknowledgements). The eroded strata were restored. Abbreviations are explained in the Figure 1 caption and stratigraphic symbols are explained in Figure 2.

transformation (Powers, 1967). No conclusion can be reached on the function of clay mineral transformation in overpressure generation in the southern Junggar Basin because of limited data. A study by Zhang et al. (2004), however, found no apparent changes of clay minerals with depth and no apparent correlation between clay mineral type and the depth and interval of overpressure occurrence. Thus, we speculate that clay mineral transformation did not contribute significantly to overpressure generation in the study area.

SIMULATION OF OVERPRESSURE GENERATION AND EVOLUTION

The purpose of our simulation is to quantitatively integrate and assess the functions of factors controlling overpressure generation and to reconstruct the evolution of subsurface pressure in the study area. A representative seismic section in the east-central part of the southern margin of the Junggar Basin was selected (Figures 1, 7). The history of evolution of this section was illustrated

by Zhuang et al. (2005). A basin-modeling computer software (see Acknowledgements) was used to simulate basin filling, three-phase fluid migration, thermal evolution, and hydrocarbon generation and expulsion in sedimentary basins and provides a two-dimensional (2-D) display of the temporal evolution of a variety of basin parameters.

Model Construction

The southern Junggar margin is characterized by complex sedimentary facies distribution and structures, formed by rapid sediment deposition, intense tectonic compression, large-scale faulting, and intense surface erosion during the Cenozoic, especially post-Miocene. A 2-D geological model was constructed from our and previous sedimentary facies interpretations (Figure 7) (Wu and Song, 1994; Zhang et al., 2004). The cross section is oriented south-southwest–north-northeast across the Qigu, Tugulu, and Hutubi anticlines and contains Jurassic to Quaternary strata and major faults that are significant to pressure evolution. In the model section, a simplified fault was placed on each anticline. On the Qigu anticline, the eroded Cenozoic strata were restored by extrapolating facies distribution and stratal thickness from adjacent areas with complete Cenozoic sections (Figure 7).

Boundary Conditions

Heat flow was assumed to be zero at both sides of the model section and positive at the base. Surface annual average temperature in the study area was assigned at the top of the section. The modern thermal gradient was estimated as 1.88°C/100 m (35.38°F/328 ft) according to the relationship $T = 0.0188Z + 20.50$, where T is temperature, and Z is depth, which was established using 156 wellbore measurements with a correlation coefficient of 0.9. Based on previous studies (Zhou and Pan, 1992; Wang et al., 2000; Qiu et al., 2002), we assumed that the thermal gradient decreased from 5 to 3°C/100 m (41 to 37.4°F/328 ft) from the Permian to the end of the Triassic and from 3 to 2°C/100 m (37.4 to 35.6°F/328 ft) from the Jurassic to the Paleogene.

Fluid flow was assumed to be zero at the sides and base of the model section. That is, there is no input of excess fluid pressure from the sides and base. Fluid pressure was assigned as 1 atmosphere (atm) (10^5 Pa) at the top surface and as the sum of atmospheric pressure and water-column pressure at the sediment-water surface.

Lithology

The sedimentary deposits were subdivided into six types (Zhang et al., 2004): sandstone, muddy sandstone, sandy mudstone, mudstone, evaporite, and coal according to their compaction behavior and permeability. The permeability of mudstones was given at first empirical values and then was calibrated by comparing the modeled and measured pressures at the same points. Lithologic and stratigraphic data from the interpreted seismic section and adjacent wells were used to establish a model lithologic column to calibrate the lithology on the 2-D model section.

Model Parameters

Many parameters were used in the simulation. Their values are determined by the specific geological conditions of the southern Junggar margin and may vary during sediment burial.

Mudstone Permeability

Mudstone permeability is very difficult to measure in the laboratory (Neuzil, 1994). However, it can be estimated through numerical pressure modeling using a variety of subsurface measurements (e.g., Luo et al., 2003). Simulation of the subsurface pressure evolution of the Anjihaihe-Ziniquanzi pressure system was conducted to obtain the mudstone permeability using the modeling method of Luo and Vasseur (1996) and Luo (1998). Their method was modified to include the effect of tectonic stress, in addition to mudstone compaction, on overpressure generation (Appendix). A simplified Kozeny-Carmen equation (Jacquin and Poulet, 1973) was used for the permeability-porosity relationship:

$$k = \psi\, \phi^n \qquad (1)$$

where k is the permeability, ψ is the permeability coefficient, ϕ is porosity, and n is 5.0, an empirical value for mudstone and sandstone.

Pressure evolution in mudstone can be modeled one-dimensionally (1-D) because mudstone has low permeability and lateral fluid flow can be ignored (Bethke, 1986). In a 1-D geologic model of well WA6 (Figure 8), basal fluid flow was assumed to be zero, and fluid pressure at the top was assumed to be 1 atm (0.1 MPa). Tectonic stress was assigned as zero at surface, increasing linearly to 30 MPa at a depth of 2000 m (6600 ft) (Sun and Tan, 1995) and constant downward (Figure 8). The horizontal compressional tectonic stress that resulted

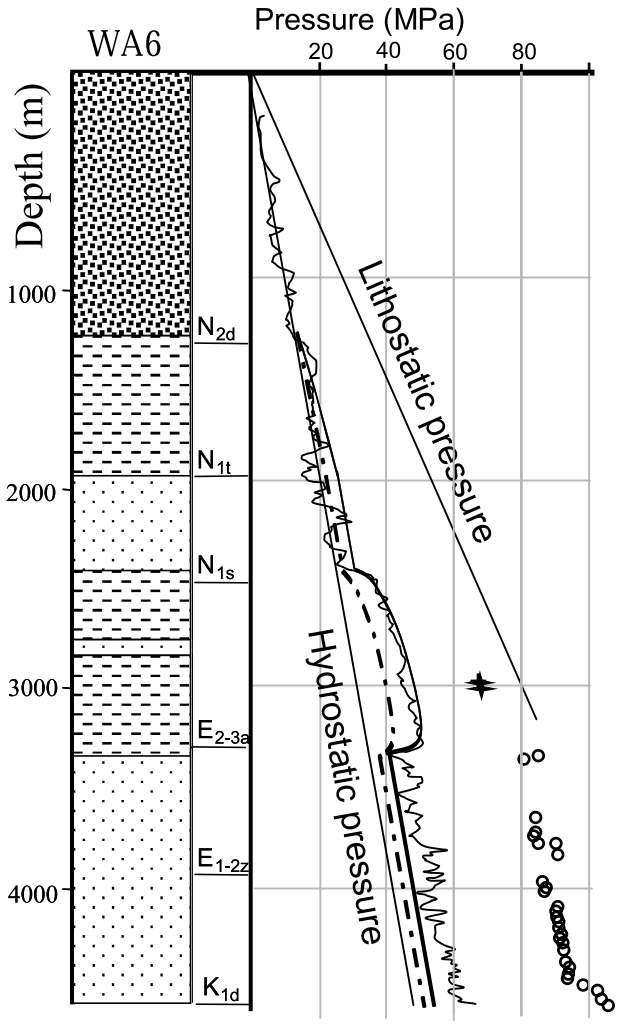

Figure 8. One-dimensional model input and output of well WA6 to obtain the mudrock permeability. The left column presents the 1-D geological model, and the right diagram shows the modeled excess pressures. The thin jagged line is excess pressure estimated from the mudrock compaction curve. The dashed line is excess pressure with only compaction from sedimentary overburden. The thick line is excess pressure with compaction from both sedimentary overburden and tectonic stress. The match between the thick line and the dotted line in the overpressure interval suggests the role that tectonic stress played in overpressure generation. See Figure 2 for explanations of stratigraphic symbols.

from the Cenozoic India–western China collision has evidently acted on the area since the Pliocene and reached a maximum value today (Zhong and Ding, 1996; Cai et al., 2000). The model also assumed that the stress that caused the present state of mudstone undercompaction, as reflected in the mudstone compaction curve, is the maximum stress experienced during sediment burial, and that the stress includes only those induced by the stratal overburden and tectonic compression. Model results suggest that the contribution of tectonic stress to overpressure generation in the Anjihaihe Formation is nearly equal to that of the stratal overburden (Figure 8). Furthermore, the modeled pressure distribution matches that estimated from the compaction curve when the permeability coefficient (λ) is 4.0 and 8.0×10^{-16} m^2 for mudrocks of the Anjihaihe and Taxihe formations, respectively (Figure 8). Thus, these two values were used in the simulation below.

Type and Content of Organic Matter

The Mesozoic and Cenozoic thick mudrocks in the study area are commonly hydrocarbon source rocks. Thus, hydrocarbon generation in the source rocks may cause pressure increase. Two major intervals of source rocks were included in the simulation: the Jurassic coals and carbonaceous shales of type III kerogen and 1.3% TOC and the lacustrine mudstones of the Eocene–Oligocene Anjihaihe Formation of type II kerogen and 0.78% TOC.

Timing of Fault Opening

Faulting might have significantly affected fluid pressure distribution in the study area. The current pressure distribution in the area suggests that some faults opened recently. Sedimentary and structural analyses by Deng et al. (2000) and fault age dating in the southern Junggar using the electron spin resonance (ESR) method by Hu et al. (2005) suggest three major episodes of faulting that occurred mainly from the early Oligocene and may last to 1.0 Ma or even later (ESR date of 0.1049 Ma). Thus, we assigned 1.65, 0.7, and 0.1 Ma as the ages of faulting in the Qigu, Tugulu, and Hutubi anticlines, respectively (Figure 8). Most faults, except those in the Qigu anticline, remain open to the present.

Other Parameters

Rock density and clay content were mainly estimated from wire-line-log data. Other rock properties, such as thermal conductivity, heat capacity, heat generation rate, decompaction rebounding coefficient, and fracturing coefficient, are adapted from the assigned values in the modeling software (Ungerer et al., 1990).

Model Calibration

Model output was consistently checked with measured pressure and temperature data. If the model results do not match the measured data, estimates of boundary conditions and rock properties were adjusted in the next model run. Temperature calibration used temperature

measurements from formation tests and well logging. Adjustment after temperature calibration was mainly to the rate of crystalline basement heat flow and, in some cases, the average thermal conductivity of rocks. Fluid pressure calibration used pressure measurements in DSTs and RFTs. Adjustment after pressure calibration was mainly to the constant in the porosity-permeability relationship (equation 1).

Model Results and Interpretation

A series of cross sections showing the distribution of excess pressure at different times demonstrate the magnitude, distribution, and evolution of subsurface fluid pressure in the area of the Qigu, Tulugu, and Hutubi anticlines in the southern Junggar margin (Figure 9).

After the deposition of Cretaceous sediments at 65 Ma, subsurface pressure was small in the north and mostly not abnormal, except the moderate overpressure in the Lower Jurassic strata (Figure 9A). However, in the south, the Lower Jurassic strata contained fairly high overpressure, and part of the Middle Jurassic strata also contained apparent overpressure. The difference in the magnitude of overpressure between north and south was probably caused mainly by rapid sediment deposition in the south.

After the Tertiary deposition at 1.65 Ma, overpressure became widespread (Figure 9B). Fairly high overpressure was present in strata underlying the mudrocks in the upper part of the Anjihaihe Formation. Faulting on the Hutubi anticline in the north readjusted the pressure distribution within some strata, forming a basically uniform distribution of excess pressure. At 0.70 Ma, moderately high overpressure was common (Figure 9C). Faulting was active in all fold belts, causing pressure readjustment among strata between the Upper Cretaceous Tonggou and Eocene–Oligocene Anjihaihe formations. The readjustment was confined to fault-connected permeable sandstones within individual anticlines because the sandstones are not laterally persistent. Faulting, however, did not destroy the seal of mudrocks in the upper Anjihaihe Formation.

At 0.5 Ma, pressure distribution was complex (Figure 9D). The Qigu anticline and its vicinity were uplifted and eroded, and faults were open, caused by the northward overthrusting of the Tianshan. As a result, fluid pressure dropped rapidly, and the excess pressure around Qigu was zero or even negative in some places. In contrast, pressure distribution in the other structures in the north was not affected by tectonic uplift in the south, and the mudrock seals in the upper Anjihaihe Formation were intact. Thus, excess pressure became higher because of rapid sediment deposition and tectonic compression associated with continuing anticline formation.

The pressure distribution at present (Figure 9E) is significantly different from that at 0.5 Ma. Uplift and erosion in the vicinity of the Qigu anticline continued, and the height of the anticline increased because of continuing overthrusting of the Tianshan. However, faults were closed on the Qigu anticline, and some dipping permeable sandstones extended laterally into the deep high-pressure zone and transmitted fluid and fluid pressure updip to generate excess pressure. In contrast, on the Hutubi anticline, the active faults cut through the mudrock seals in the upper Anjihaihe Formation, causing a pressure drop to hydrostatic values in the underlying sandstones. The interbedded mudrocks, however, still contain a certain degree of overpressure.

DISCUSSION

Sandstone compaction does not commonly generate overpressure because the large resistance of sand grains prohibits severe porosity reduction and preserves a fairly high permeability for rapid fluid flow. Overpressure in permeable sandstones, thus, was commonly believed to have transmitted from adjacent mudrocks (Magara, 1978). Faulting, however, may hydrodynamically connect isolated permeable sandstones, and folding may cause a permeable reservoir contact with mudstones at different burial depths and different states of compaction and overpressuring (Luo et al., 2000, 2003). Pressure will then readjust to form a complex distribution. As a result, sandstones may contain much different pressure than adjacent mudrocks.

Sediment compaction by stratal overburden is the basic requirement for overpressure generation (Fertl, 1976; Luo and Vasseur, 1992). Tectonic stressing also causes sediment compaction and, additionally, changes in sediment physical properties, such as density increase and change in sediment compaction trend. In the study area, the contribution of sediment compaction by stratal overburden and tectonic compression to excess pressure is limited, with a pressure coefficient less than 1.6.

Open faults greatly change fluid dynamics conditions in the sediments by connecting hydraulically different pressure systems. In the southern Junggar Basin, the open faults are current or geologically recent. If a shallow, hydrostatically pressured system is connected with a deep overpressured system, both systems will

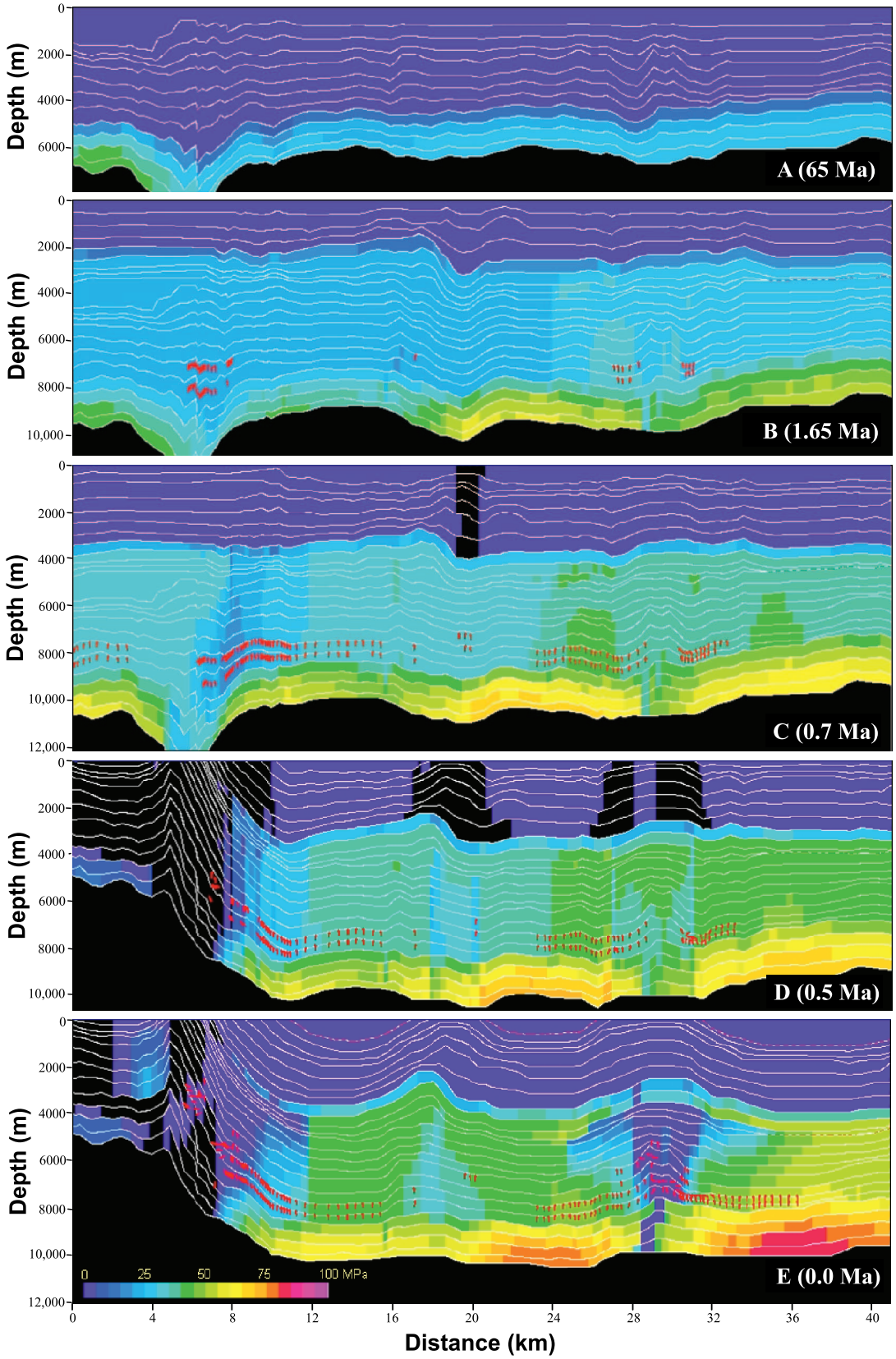

Figure 9. Model results showing overpressure generation and evolution along a north-south cross section in the east-central part of the southern margin of the Junggar Basin at different times of the basin history (A–E). Faulting and folding since 0.7 Ma have caused complex overpressure distribution. The geological model used in the simulation is shown as Figure 7C. See text for discussion.

become hydrostatic, as evidenced by the hydrostatically pressured deep and shallow permeable systems in the Hutubi anticline. However, if the connected shallow system is compartmentalized, the deep and shallow systems will form a unified new overpressured system.

Folding will cause differential sediment deposition and surface erosion across an anticline. A dipping mudrock bed will be subject to lesser overburden in the updip direction, and the degree of undercompaction and overpressuring of the mudrock will then decrease in the updip direction. As a result, the amount of fluid and pressure transmitted to a dipping permeable sandstone bed from the adjacent overpressured mudrocks will differ laterally within the sandstone. The lateral difference will cause pressure transmission and fluid flow within the sandstone to significantly change its pressure distribution (Luo et al., 2000; Yardley and Swarbrick, 2000) and, in some cases, generate extremely high overpressures in the shallow updip part of the sandstone, as evidenced in the Anjihai anticline.

SUMMARY

The widespread high overpressure in the Mesozoic and Cenozoic strata in the southern margin of the Junggar Basin is thought to be closely related to the northward compression from the northern Tianshan and associated structural deformation in the margin. Numerical modeling of pressure generation and evolution suggests that faulting and stratal tilting associated with folding are the most significant factors in overpressure generation of permeable sandstone. The extremely high overpressure (with a pressure coefficient up to 2.4) is interpreted to have resulted from the superimposition of allogenically transmitted pressure along faults and dipping permeable sandstones on background high pressure, which was generated by compaction and tectonic compression.

APPENDIX: INTRODUCTION OF TECTONIC STRESS IN THE HYDRODYNAMIC EQUATION

The influence of tectonic stress was not considered in our former basin numerical model (Luo and Vasseur, 1992; Luo, 1998). In this model, the finite-element method is used to solve the hydrodynamic and thermal equations. The tectonic stress as well as compaction of sediments, geometry, and deformation of basin, hydraulic process, and geothermal field are coupled by an iterative circulation method (Luo and Vasseur, 1992; Luo, 1998). In the model, the water-rock interaction and other possible chemical diagenesis in sediments are neglected.

In sedimentary basins, the tectonic stress acts generally in horizontal directions. The stress state in rocks may be interpreted as the composition of two stress fields: one is the gravity stress field, and another is the tectonic stress field. If one of the horizontal principal stresses of the gravity stress field is in the same direction as the tectonic stress, then we have

$$\begin{cases} \sigma_v = \rho_{\bar{b}} g z \\ \sigma_H = \upsilon \times \sigma_v + \sigma_T \\ \sigma_h = \upsilon \times \sigma_v \end{cases} \quad (2)$$

where υ is stress ratio coefficient; σ_v is the vertical stress; σ_H and σ_h are, respectively, the maximum and minimum horizontal stresses; σ_T is the tectonic stress; $\rho_{\bar{b}}$ is the average density of rocks; g is the gravity acceleration; and z is the burial depth.

To take the influence of tectonic stress on sediment compaction into account, the concept of average effective stress $\bar{\sigma}'$ was induced in

$$\bar{\sigma}' = \frac{1}{3}(\sigma_v + 2\upsilon\sigma_v + \sigma_T) - P \quad (3)$$

where P is the pore pressure. Substituting equation 3 into the relationship between porosity and effective stress proposed by Smith (1971), we have

$$\phi = \phi_0 e^{-\frac{c}{[\rho_b(1+2\upsilon)/3-\rho]g}\bar{\sigma}'} \quad (4)$$

where c is the compaction coefficient obtained from a porosity-depth relation, ϕ_0 is the porosity of sediments at deposition surface, and ρ is the density of the pore fluid.

When vertical stress is replaced by average stress, the hydrodynamic formula becomes (Luo and Vasseur, 1992)

$$(\beta\phi + \frac{\alpha_\phi'}{1-\phi})\frac{dP}{dt} = \frac{1}{\rho}\nabla \times \left[\frac{k\rho}{\mu}(\nabla P - \rho\vec{g})\right] + \frac{\alpha_\phi'}{1-\phi}\frac{d\bar{\sigma}}{dt} + \alpha\phi\frac{dT}{dt} + Q \quad (5)$$

where $\bar{\sigma} = \bar{\sigma}' + P$ is average stress, and α_ϕ' is the porosity compressibility. When the stress ratio is a constant, α_ϕ' may be presented as

$$\alpha_\phi' = -\frac{\phi c}{[\rho_b(1+2\upsilon)/3-\rho]g} \quad (6)$$

REFERENCES CITED

Audet, D. M., 1995, Mathematical modeling of gravitational compaction and clay dehydration in thick sediment layers: Geophysics Journal International, v. 122, p. 283–298.

Audet, D. M., and J. D. C. McConnell, 1992, Forward modeling of porosity and pore pressure evolution in sedimentary basins: Basin Research, v. 4, p. 147–162.

Bethke, C. M., 1986, Inverse hydrologic analysis of the distribution and origin of Gulf Coast–type geopressured zones: Journal of Geophysical Research, v. 91, p. 6535–6545.

Byerlee, J., 1990, Fracture, overpressure and fault normal compression: Geophysical Research Letters, v. 17, p. 2109–2112.

Byerlee, J., 1993, Model for episodic flow of high-pressure water in fault zones before earthquakes: Geology, v. 21, p. 303–306.

Cai, Z. X., F. J. Chen, and Z. Y. Jia, 2000, Types and tectonic evolution of Junggar Basin (in Chinese): Earth Science Frontiers, v. 7, p. 431–440.

Davis, D. M., J. Suppe, and F. A. Sahken, 1983, Mechanics of fold-and-thrust belts and accretionary wedges: Journal of Geophysical Research, v. 88, p. 1153–1172.

Deng, Q. D., X. Y. Feng, and P. Z. Zang, 2000, Active tectonics of

the Chinese Tianshan Mountains (in Chinese): Beijing, Seismological Press, 385 p.
Ding, G. Y., W. B. Cai, P. Q. Yu, and G. L. Xie, 1991, Lithospheric dynamics of China (in Chinese): Beijing, Seismological Press, 600 p.
Fertl, W. H., 1976, Abnormal formation pressure, implication to exploration, drilling, and production of oil and gas reservoirs: Amsterdam, Elsevier, p. 1–382.
Grauls, D. J., and J. M. Baleix, 1994, Role of overpressures and in situ stresses in fault-controlled hydrocarbon migration: A case study: Marine and Petroleum Geology, v. 11, p. 734–742.
Hu, L., D. F. He, and D. G. Hu, 2005, Electron spin resonance dating of the late Cenozoic deformation of the Huoerguosi-Manas-Tugulu reverse faults along southern edge of Junggar Basin (in Chinese): Acta Geoscientica Sinica, v. 26, p. 121–126.
Jacquin, C., and M. Poulet, 1973, Essai de restitution des conditions hydrodynamiques renant dans un bassins sedimentaire au cours de son evolution: Revue de l'Institut Français du Petrole, v. 28, p. 269–297.
Kuang, J., 1993, The superpressure mud seams in the southern margin of the Junggar Basin and their significance in structure geology (in Chinese): Experimental Petroleum Geology, v. 15, p. 168–173.
Law, B. E., and W. Dickinson, 1985, Conceptual model for origin of abnormally pressured gas accumulation in low-permeability reservoirs: AAPG Bulletin, v. 69, p. 1295–1304.
Li, T. J., 2004, The overpressure and its generation in the south edge of Junggar Basin (in Chinese): Geological Sciences, v. 39, p. 234–244.
Li, Z. Q., G. S. Chen, J. Y. Guo, and Y. L. Chi, 2001, Basic geologic character of the abnormal formation overpressure in the western part of southern fringe of Junggar Basin (in Chinese): Petroleum Geology and Experiment, v. 23, p. 47–51.
Luo, X. R., 1998, Numerical basin modeling: Conception, composition and verification (in Chinese): Oil and Gas Geology, v. 19, p. 196–204.
Luo, X. R., and G. Vasseur, 1992, Contributions of compaction and aquathermal pressuring to geopressure and the influence of environmental conditions: AAPG Bulletin, v. 76, p. 1550–1559.
Luo, X. R., and G. Vasseur, 1996, Geopressuring mechanism of organic matter cracking: numerical modeling: AAPG Bulletin, v. 80, p. 856–874.
Luo, X. R., J. H. Yang, and Z. F. Wang, 2000, The overpressuring mechanisms in aquifers and pressure prediction in basins (in Chinese): Geological Review, v. 46, p. 6–10.
Luo, X. R., W. L. Dong, J. H. Yang, and W. Yang, 2003, Overpressuring mechanisms in the Yinggehai Basin, South China Sea: AAPG Bulletin, v. 87, p. 629–645.
Magara, K., 1978, Compaction and fluid migration: Practical petroleum geology: Amsterdam, Elsevier Scientific Publishing Company, 319 p.
Mudford, B. S., and M. E. Best, 1989, Venture gas field, offshore Nova Scotia: Case study of overpressuring in region of low sedimentation rate: AAPG Bulletin, v. 73, p. 1383–1396.
Nelson, M. R., R. McCaffrey, and P. Molnar, 1987, Source parameters for 11 earthquakes in the Tien Shan, central Asia, determined by P and SH waveform inversion: Journal of Geophysical Research, v. 92, p. 12,629–12,648.
Neuzil, C. E., 1994, How permeable are clays and shales?: Water Resources Research, v. 30, p. 145–150.
Neuzil, C. E., 1995, Abnormal pressures as hydrodynamic phenomena: American Journal of Science, v. 295, p. 745–786.
Neuzil, C. E., and D. W. Pollock, 1983, Erosional unloading and fluid pressures in hydraulically ''tight'' rocks: Journal of Geology, v. 91, p. 179–193.
Osborne, M. J., and R. E. Swarbrick, 1997, Mechanisms for generating overpressure in sedimentary basins: A reevaluation: AAPG Bulletin, v. 81, p. 1023–1041.
Powers, M. C., 1967, Fluid-release mechanism in compacting marine mudrocks and their importance in oil exploration: AAPG Bulletin, v. 51, p. 1240–1254.
Qiu, N. S., H. B. Yang, and X. L. Wang, 2002, Tectono-thermal evolution of western Junggar Basin, northwest China (in Chinese): Chinese Journal of Geology, v. 37, p. 423–429.
Smith, J. E., 1971, The dynamics of shale compaction and evolution of pore-fluid pressures: Mathematical Geology, v. 3, p. 239–263.
Spencer, C. W., 1987, Hydrocarbon generation as a mechanism for overpressuring in Rocky Mountain region: AAPG Bulletin, v. 71, p. 368–388.
Sun, Y., and C. X. Tan, 1995, An analysis of present-day regional tectonic stress field and crustal movement trend in China (in Chinese): Journal of Geomechanics, v. 1, p. 1–12.
Swarbrick, R. E., and M. J. Osborne, 1998, Mechanisms that generate abnormal pressures: An overview, *in* B. E. Law, G. F. Ulmishek, and V. I. Slavin, eds., Abnormal pressures in hydrocarbon environments: AAPG Memoir 70, p. 13–34.
Ungerer, P., J. Burrus, B. Doligez, Y. Chenet, and F. Bessis, 1990, Basin evaluation by integrated two-dimensional modeling of heat transfer, fluid flow, hydrocarbon generation, and migration: AAPG Bulletin, v. 74, p. 309–335.
Wang, S. J., S. B. Hu, and J. Y. Wang, 2000, The characteristics of heat flow and geothermal fields in Junggar Basin (in Chinese): Chinese Journal of Geophysics, v. 43, p. 771–779.
Wu, X. Z., and Z. G. Song, 1994, Tertiary reservoir characteristics and influence factor in western part of south margin of Junggar Basin (in Chinese): Acta Petrolei Sinica, v. 15, p. 23–30.
Wu, X. Z., L. H. Wang, and Z. L. Song, 2000, The relation between structural stress field and hydrocarbon migration and accumulation in southern margin of Junggar Basin (in Chinese): Xinjiang Petroleum Geology, v. 21, p. 97–100.
Xu, G. S., J. C. Kuang, J. L. Li, and L. R. Dang, 2000, Research on the genesis of abnormal high pressure in the foreland basin to the north of Tianshan (in Chinese): Journal of Chengdu University of Technology, v. 27, p. 255–262.
Yardley, G. S., and R. E. Swarbrick, 2000, Lateral transfer: A source of additional overpressure?: Marine and Petroleum Geology, v. 17, p. 523–537.
Yin, G. H., Y. D. Mai, B. J. Jiang, L. Z. Xie, Y. G. Zhang, M. Ge, Y. Y. Wang, and H. J. Li, 1999, Study on deformation survey by GPS and fault activity in Dushazi, Xinjiang (in Chinese): Inland Earthquake, v. 13, p. 345–351.
Zeng, W. Q., J. H. Zheng, C. L. Feng, and X. H. Hu, 2000, The drilling techniques used in high difficult deep boreholes on pre-mountain structures in the south margin of the Zhungaer Basin (in Chinese): Natural Gas Industry, v. 20, p. 44–47.
Zha, M., W. H. Zhang, and J. X. Qu, 2000, The character and origin of overpressure and its explorational significance in Junggar Basin (in Chinese): Petroleum Exploration and Development, v. 7, p. 31–35.
Zhang, L., Q., X. R. Luo, D. F. He, L. J. Liu, and J. D. Jia, 2004, Sequence boundaries of the Lower Cretaceous, southern Junggar Basin (in Chinese): Acta Sedimentologica Sinica, v. 22, p. 636–643.
Zhong, D. L., and L. Ding, 1996, Rising process of the Qinghai-Xizang (Tibet) Plateau and its mechanism: Science in China, Series D, v. 28, p. 289–295.
Zhou, Z. Y., and C. C. Pan, 1992, Paleotemperature analysis methods and their application in sedimentary basins (in Chinese): Guangzhou, Guangdong Science and Technology Press, 182 p.
Zhuang, X., W. Chen, and X. Wang, 2005, Structural analysis and a preliminary model for the Tugulu anticline in the south margin of Junggar Basin: Geotectonica et Metallogenia, v. 29, p. 223–226.